10

The effect of powerful ultrasonic assistance during pressing on structural and luminescent properties of YAG : Ce^{3+} ceramics

© D. Valiev, O. Khasanov, E. Dvilis, V. Paygin, S. Stepanov

Tomsk Polytechnic University, Tomsk, Russia

e-mail: rubinfc@tpu.ru

Received October 25, 2022
Revised January 13, 2023
Accepted January 16, 2023

Yttrium aluminum garnet (YAG) ceramics doped with Ce^{3+} was prepared by dry compaction using the common uniaxial pressing under powerful ultrasound assistance (PUA). The structure and luminescent properties of sintered ceramics were investigated. It was demonstrated that the powerful ultrasonic assistant during the dry pressing has a positive effect on the structural and luminescent characteristics of YAG : Ce^{3+} ceramics. The sintered material consolidation is very intensive accompanied by a decrease in the number of pores and grain growth at a sintering temperature of 1650 °C. The luminous efficiency of YAG : Ce^{3+} ceramics vary from 120 to 219 lm/W (without ultrasound treatment) and from 120 to 250 lm/W (prepared with ultrasound conditions) closely related with the phase purity and implicitly with sintering temperature. It was demonstrated the positive effect of PUA on the thermal properties of ceramics.

Keywords: YAG : Ce ceramics, powerful ultrasonic compaction, luminescent properties, elastic-plastic properties, luminous efficiency.

DOI: 10.61011/EOS.2023.05.56510.71-22

1. Introduction

One of the latest directions in the field of lighting engineering and LED light sources is the use of luminescent ceramics as a radiation converter [1–5]. The advantages of luminescent ceramics as a solid-state radiation converter in white LED are based on the opportunity of varying thermal, optical, and mechanical properties. This is important for extreme operating conditions: high pumping flows, high temperatures with long service life [6,7]. The thermal conductivity of dense ceramics is almost 100% of theoretical, which is much higher than that of transducers based on phosphor powders dissolved in epoxy resin or silicone matrix [8,9]. These properties allow to convert incident radiation faster and more efficiently with minimal energy dissipation in the material [10,11].

The most common optical material used in white LEDs is Ce^{3+} activated YAG ceramic due to its excellent mechanical, thermal and chemical properties [12–15]. YAG : Ce^{3+} ceramics can be obtained by traditional pressing methods followed by sintering in air or vacuum [16–18]. The choice of a suitable pressure molding technology is of decisive importance for the sintering of luminescent ceramics. The widely used „traditional" ceramic molding methods have problems with the complexity of the process, poor quality of finished products and environmental pollution. As the quality of ceramics improves, further enhancement of the physicochemical properties becomes more and more laborious. To date, all opportunities for increasing the synthesis efficiency of phosphor ceramics by empirical selection of combinations of starting materials and technological methods have been practically exhausted. The existing understanding of processes in phosphor-based ceramics at the conversion of UV radiation from an LED chip into visible light is also insufficient to predict areas for improvement.

A large number of publications are devoted to a detailed description of studies of luminescent characteristics depending on the composition of the initial ceramic or a description of the results achieved under the selected technological sintering conditions. In almost all the published papers, cerium ions are considered as the ground luminescence center, sometimes with rare-earth ions as coactivators. Thus, it can be assumed that the luminescent characteristics of phosphor ceramics for white LEDs are determined not only by the initial composition of the sintered components, but also by the technological conditions and sintering modes. Development of new approaches to the study of phosphors for LEDs is required.

In this regard, it is relevant to use methods that do not require large expenditures, do not use potentially polluting plasticizers and allow obtaining ceramics with a uniform density and minimal residual porosity. These methods include, in particular, high-power ultrasonic (US) treatment during compaction followed by a sintering process [19–22]. The total stress of the deformable powder material is regularly redistributed in the matrix. In the molding process, a powerful ultrasonic effect is used to regularly redistribute the particles of the phosphor powder. The distribution of pressure and density over the molding volume becomes regular due to a decrease in near-wall friction during ultrasonic treatment. The packing density of the powder particles and, as a result, a higher compaction density, even of complex geometry, is achieved by reducing the friction

Values of relative density and porosity of YAG:Ce^{3+} ceramics

Molding pattern	T sintering, °C	Density, g/cm^3	Rel. density, %	Rel. porosity, %
without US	1550	3.74	82.1	17.9
	1600	4.11	90.1	9.9
	1650	4.47	98.1	1.9
	1700	4.44	97.5	2.5
US	1550	3.78	82.9	17.1
	1600	4.21	92.3	7.7
	1650	4.54	99.6	0.4
	1700	4.41	96.8	3.2

between the particles. The phase composition and structure of molded ceramics by the ultrasonic method depend on such conditions and parameters as pressure, power and duration of treatment. It has been specified that the use of ultrasonic exposure during the molding of powder mixtures significantly affected the grain size and phase composition of sintered ceramics. In the process of ultrasonic exposure, a homogeneous structure is formed with the preservation of nanosized grains and subgrains with the stabilization of the high-temperature phase [21].

There are only a few papers devoted to the effect of ultrasonic exposure on structural and luminescent properties. However, this approach is limited to processing only according to the phosphor preparation procedure. In [23] the positive effect of ultrasonic treatment on the luminescent characteristics of Y_2SiO_5:Ce phosphors was demonstrated. The radiation intensity of the phosphors was improved from 105% (without US treatment) to 151% with US treatment, which may be related to phase purity and indirectly to the annealing temperature.

This paper is devoted to studying the effect of high-power ultrasonic treatment on the structural and luminescent properties of ceramics based on yttrium-aluminum garnet activated by cerium ions. The technology of ultrasonic molding of the phosphor powder was used in the paper. The powder molding technology with powerful US in the axial and transverse directions allows the production of ceramics with optimal characteristics and improved light output. The use of ultrasonic exposure conditions during the molding of the phosphor powder allowed to reduce the friction between the powder particles and the mold wall, reduce the gradient of residual stresses, and achieve the absence of warpage and regular shrinkage during sintering. All the indicated factors lead to an increase in the relative density and light output of YAG:Ce ceramics.

2. Examined samples and experimental procedure

2.1. Manufacture of YAG:Ce^{3+} ceramics

A homogeneous mechanical mixture of chemically pure reagents was used as initial powders Al_2O_3 (99.99%), Y_2O_3 (99.99%), CeO_2 (99.99%) (CUAS — Chongqing University of Arts and Sciences, China). The sizes of the structural elements of the initial YAG:Ce precursor powder range from 271 nm to 31.0 μm. The average size of structural elements is 2.01 μm. The synthesis procedure and morphology of phosphor powders are described in more detail in [24–26]. The cerium content in the YAG powder was 0.06 wt.%. The phosphor powder was molded by cold static uniaxial molding in a steel mold with simultaneous exposure to ultrasonic vibrations at a pressure of 400 MPa on an IP-500 AVTO automatic press (ZIPO, Russia) [20]. The power of the ultrasonic waves of the driving oscillator was 800 W. Sintering of YAG:Ce^{3+} ceramics was carried out in a high-temperature LHT 02/18 furnace (Nabertherm, Germany) in an air atmosphere at temperatures of 1550–1700 °C with a controlled heating and cooling rate of 200 °C/min. The holding time at a given sintering temperature was 8 h. Cylindrical YAG:Ce ceramics was obtained with a height of approximately 1.5 mm and a diameter of approximately 8.5 mm. Density values were estimated by measuring the mass and linear dimensions of ceramics. Further studies of ceramics were carried out after mechanical polishing of the end surfaces on an EcoMet 300 Pro grinding and polishing complex (Buehler, Germany) using Kemix diamond suspensions (Kemika, Russia). The parameters of the obtained ceramic samples are given in the table.

2.2. Experimental methods

X-ray diffraction (XRD) analysis was performed on the XRD-7000S X-ray diffractometer (Shimadzu, Japan). The results of X-ray diffraction analysis were interpreted using the free software „PowderCell“ and the international crystallographic database „*PDF* 4“. Photoluminescence (PL) spectra were recorded on an AvaSpec-3648 fiber-optic spectrometer (spectral range 200–1100 nm). A blue LED chip was used to excite luminescence (λ_{ex} = 447 nm, FWHM 20 nm, energy flux 16 mW/cm^2). The PL spectra of the ceramic samples were recorded in the reflection geometry. The integration time was 1 s. We also measured the luminescence decay kinetic characteristics of YAG:Ce^{3+} ceramics upon excitation by an LED chip

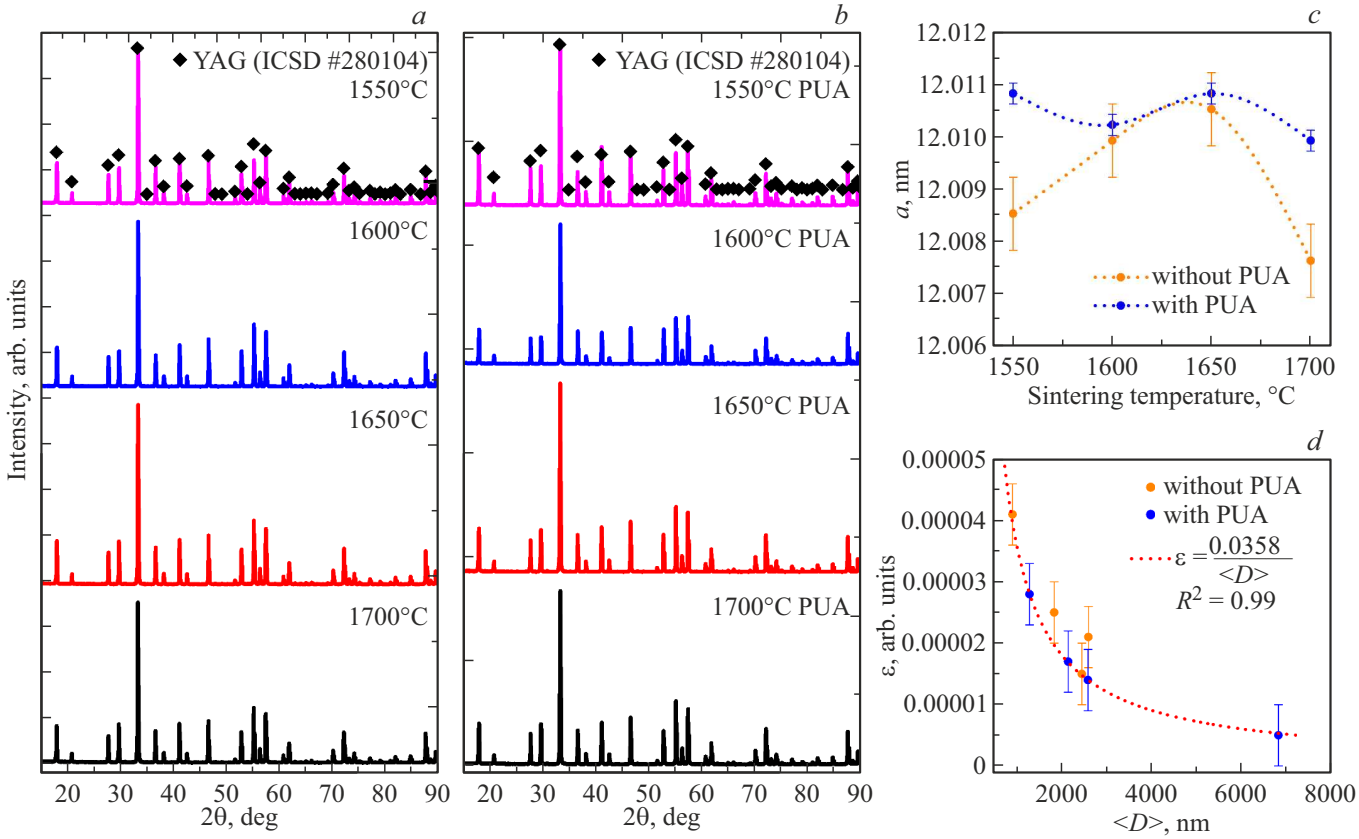

Figure 1. X-ray diffraction patterns of YAG:Ce ceramics without (a) and with (b) ultrasonic treatment at different sintering temperatures; dependence of the lattice cell parameter a on the sintering temperature (c) and relative microstrains ε on the average size of coherent scattering areas (crystallite size D) (d).

($\lambda_{ex} = 452$ nm, $\tau_{1/2} \sim 15$ ns). Luminescence was recorded through an MDR-204 monochromator, PMT Hamamatsu 10720-20 using a Tektronix DPO-3033 digital oscilloscope (300 MHz). The time resolution of the system was 2 ns.

3. Results and discussion

3.1. X-ray diffraction analysis and morphology

XRD analysis confirmed that the ceramic samples have a stoichiometric yttrium aluminum garnet with a cubic structure. No secondary foreign phases were found. All reflections present in the diffraction patterns are phase characteristics of yttrium aluminum garnet. Fig. 1 a, b shows the experimental and reference (ICSD№280104) data.

An evaluation of the parameters of the crystal structure did not reveal significant differences between the YAG:Ce^{3+} ceramics obtained under different conditions and a stable relationship with the manufacturing modes. The lattice cell parameter a for all studied ceramic samples is in the range from 12.0076 to 12.0108 nm (Fig. 1, c). However, the scatter of parameter values for different sintering modes turned out to be smaller without significant deviations for samples prepared under US treatment.

The parameters of the coherent scattering areas of the crystal structure of ceramics fabricated under US exposure, estimated by the Hall-Williamson method, are inversely proportional with a constant coefficient $D = 0.0358$ nm and a high approximation accuracy (minimum 99.9%). This indirectly confirms the ultrasonic relaxation effect on ceramics and is in a state of energy equilibrium in any sintering mode (Fig. 1, d). Ceramics fabricated without US showed some deviation from this dependence in the direction of increasing microstresses, which indicates the retention in these samples of residual (after molding) or induced (during the synthesis of YAG:Ce^{3+}) mechanical stresses even after high-temperature treatment for 8 h.

An analysis of the structural morphology of the YAG:Ce^{3+} samples based on the results of scanning electron microscopy (SEM) shows a mixed character of the fracture of sintered ceramics (Fig. 2, a).

With an increase in the specified sintering temperature from 1550 °C to 1700 °C, intergranular destruction decreases, and transcrystalline destruction increases. For YAG:Ce ceramics, there is no formation of a dense structure at consolidation temperatures of 1550 °C and 1600 °C. The sintered ceramic has a large number of pores, and the grain size remains at the level of several

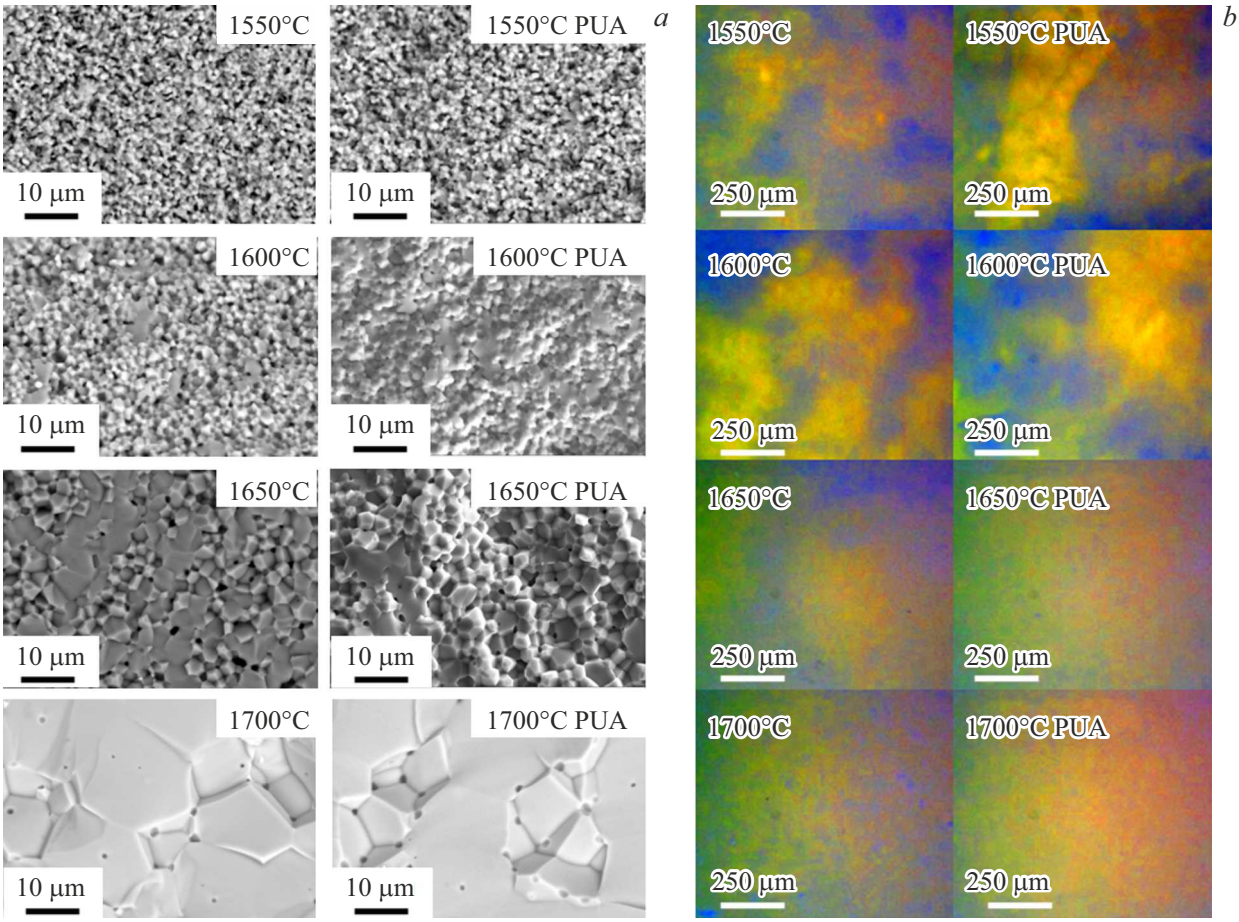

Figure 2. Images of samples of YAG:Ce^{3+} ceramics sintered at different temperatures, fabricated under and without ultrasonic treatment: obtained using SEM (a) and an optical microscope under blue LED excitation, $\lambda_{ex} = 447$ nm (b).

micrometers, which corresponds to the average particle size of the initial powder. Consolidation of sintered ceramics proceeds very intensively, accompanied by a decrease in the number of pores and grain growth at a temperature of 1650:Ce°C. The process of compaction of sintered ceramics YAG:Ce^{3+} slows down sharply at a temperature of 1700°C. Significant grain growth occurs, leading to the transition of intergranular residual pores into the volume of grains.

The homogeneity of the distribution of luminescence centers was estimated from the luminescence images shown in Fig. 2, b obtained using an optical microscope with direct excitation of YAG:Ce ceramics by LED radiation ($\lambda_{ex} = 447$ nm). With an increase in the sintering temperature, the homogeneity of radiation from the surface of the YAG:Ce^{3+} ceramics increases due to a decrease in the number of blue areas associated with reflected radiation. There is a positive effect when comparing images of ceramics prepared under and without ultrasonication at the same sintering temperature. Only a small area of reflective zones is visible. A more regular distribution of cerium ions in YAG:Ce^{3+} ceramics is directly related to the US effect.

3.2. Spectral-kinetic characteristics

Fig. 3, a shows the luminescence spectra in the spectral area 375–800 nm. YAG:Ce^{3+} ceramics without and with the use of preliminary ultrasonic treatment were excited by an LED chip with a wavelength of 447 nm. Several radiation bands are recorded in the PL spectra.

The ground broad luminescence band falls on the spectral range 460–750 nm with a maximum of the luminescence band $\lambda_{em} = 540$ nm. The nature of the radiation band corresponds to the $5d$–$4f$ emission transitions in the cerium ion [27–30]. Weak luminescence bands of YAG:Ce^{3+} ceramics in the spectral range 400–470 nm with a maximum of the luminescence band $\lambda_{em} \sim 440$ nm may be due to YAl antisite defects and charged oxygen vacancies (F^+- and F centers) [31]. The position of the ground luminescence band is in the range from 515 to 560 nm in all the observed YAG:Ce ceramics. The half-widths of the luminescence bands of all the studied ceramics are close and differ little depending on the sintering temperature.

The kinetic curves of the luminescence decay of the YAG:Ce^{3+} ceramics upon excitation by the radiation of an LED chip ($\lambda_{ex} = 452$ nm) (Fig. 3, b) have been studied. It

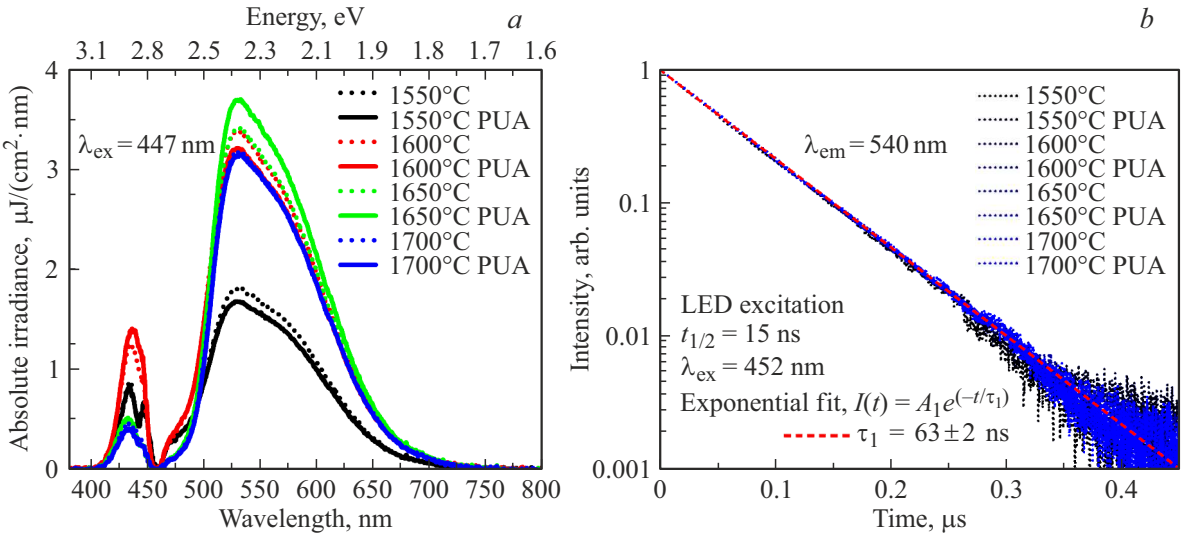

Figure 3. PL spectra of (*a*) YAG:Ce ceramics excited by blue LED radiation ($\lambda_{ex} = 447$ nm). Luminescence decay kinetics of YAG:Ce ceramics (*b*).

can be seen that the decay kinetics can be approximated by a monoexponential function. The characteristic decay times for all ceramic samples are within 63±2 ns.

As follows from the presented results, the luminescence upon photoexcitation has a short-lived component. However, the characteristic luminescence decay times differ insignificantly within the error. Probably, this means that the luminescence centers are the same in all YAG:Ce^{3+} ceramics. Radiation occurs at a radiative transition from the same excited state.

The luminous efficiency of converting excitation into visible light is the main characteristic of phosphor ceramics required for its use in a light source. The light output was evaluated by measuring the luminescence energy spectra ($F_e(\lambda)$) [24,32]. The calculations were carried out according to the following equation:

$$\eta = 6831\text{m/W}\,\frac{\int_{400}^{760} F_e(\lambda)\nu(\lambda)d\lambda\,[\text{W}]}{P_{\text{LED}}\,[\text{W}]},$$

where P_{LED} — LED electric power, $F_e(\lambda)$ — energy luminescence spectra of YAG:Ce^{3+}, $\nu(\lambda)$ ceramics — relative spectral efficiency.

The light output of YAG:Ce^{3+} ceramics under and without ultrasonic exposure was measured using an integrating sphere. LED with a wavelength of $\lambda_{max} = 447$ nm served as a source of radiation exciting the luminescence. The maximum value of light output at a temperature of 1650 °C is higher for ceramics prepared under ultrasonic exposure, and is approximately 250 lm/W (Fig. 4, *a*).

To evaluate the temperature-dependent luminescence properties of sintered YAG:Ce^{3+} ceramics, the samples were heated to complete temperature quenching of the PL by direct measurement of luminescence during heating. For PL excitation, LED emitting at a wavelength of 447 nm was used. Fig. 4, *b* shows the amplitude dependences of the PL intensity measured during heating in the temperature range from 23 °C to 600 °C of YAG:Ce^{3+} ceramic samples manufactured with and without ultrasonic treatment at a sintering temperature of 1650 °C. The samples obtained under the indicated synthesis conditions have the maximum luminescence conversion efficiency (Fig. 4, *a*). It can be seen from the obtained results that ceramics can be operated up to temperatures of approximately 500 °C. The positive effect of ultrasonic exposure should be underlined during ceramic sintering on the temperature stability of luminescence. Thus, for YAG:Ce ceramics subjected to ultrasonic treatment, thermal quenching of luminescence begins only after 150 °C, in contrast to YAG:Ce^{3+} ceramic samples manufactured without ultrasonic treatment, for which luminescence quenching is recorded already at 50 °C. After cooling, the luminescence parameters for the studied ceramic samples returned to the initial ones. There was no thermal degradation of luminescent properties in the operating temperature range.

There is a negative linear dependence between the luminescence efficiency and reflection at a wavelength of 447 nm, which is most reliable for samples prepared without ultrasonic treatment (Fig. 5, *a*). This suggests the existence of a dependence of these values on the residual porosity of the ceramic. Indeed, their comparison showed that the reflection with high reliability (not less than 99%) linearly depends on the residual porosity (Fig. 5, *b*). The minimum reflectance value for a non-porous material (8.89%) is equal to the Fresnel-calculated reflectance at the air-YAG:Ce^{3+} interface. The dependence of the light output of YAG:Ce^{3+} ceramics prepared without ultrasonic treatment on their porosity is linear with high reliability (minimum 99%) (Fig. 5, *c*).

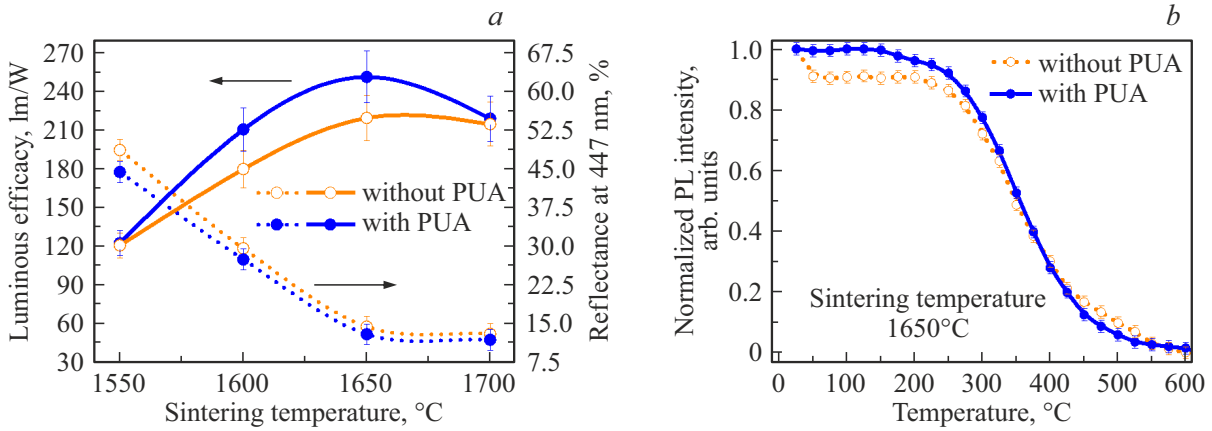

Figure 4. Dependences of the reflectance and light output on the sintering temperature YAG:Ce^{3+} ceramics (*a*). Temperature dependence of the PL intensity of YAG:Ce^{3+} ceramics under and without ultrasonic treatment (*b*).

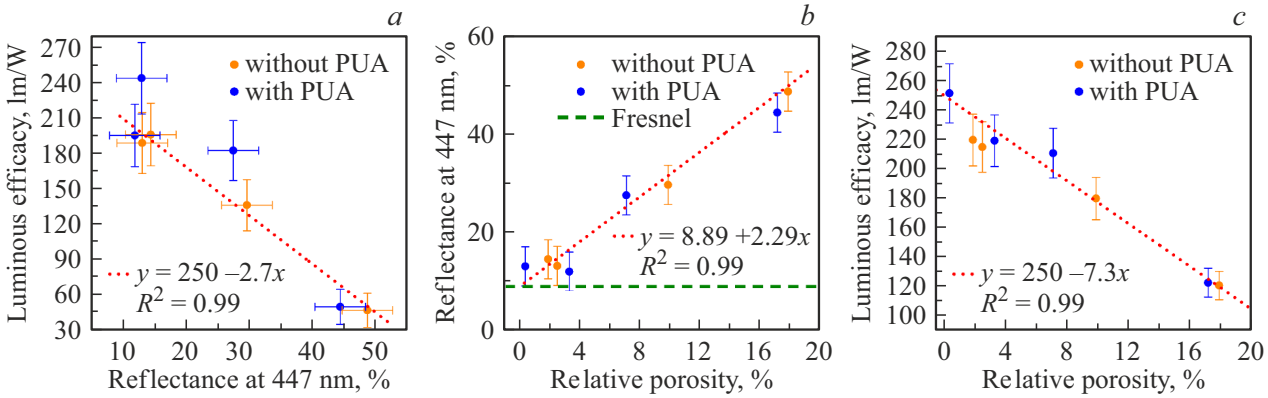

Figure 5. Dependences of the light output on the value of the reflectance at a wavelength of 447 nm (*a*), the reflectance at 447 nm (*b*) and the light output (*c*) depending on the relative porosity.

Conclusion

The YAG:Ce phosphors were obtained by the solid-phase reaction method. Intense ultrasound applied during dry molding of YAG:Ce powder leads to an increase in the relative density and grain size, and a decrease in the pore size of traditionally sintered YAG:Ce-ceramics.

A positive effect of ultrasonic treatment on the luminescent properties of ceramics was revealed. In the structure of YAG:Ce ceramics sintered with and without ultrasonic treatment, there were no changes after analysis of the XRD analysis data. Heat treatment at temperatures from 1650 °C to 1700 °C leads to a decrease in ceramic porosity and the formation of melts. The PL spectra show two bands in the blue (300–400 nm) and yellow-green regions of the spectrum (500–700 nm). The nature of the radiation bands is related to the intrinsic defects YAG:Ce of the ceramics and the emission transition in Ce^{3+} ions. The luminescence decay time of YAG:Ce ceramics with and without ultrasonic treatment practically does not change and is described by a monoexponential function ($\tau_1 \sim 63 \pm 2$ ns). The luminescence conversion efficiency of YAG:Ce ceramics varies from 120 to 219 lm/W (without US treatment) and from 120 to 250 lm/W (with US treatment), which is closely related to the phase purity and indirectly to the sintering temperature. A positive effect of ultrasonic treatment on the thermal properties of ceramics is shown. The PL intensity practically does not change at an annealing temperature up to 250 °C. It has been established that the reflectance in the ground excitation band and the light output of YAG:Ce ceramics directly depend on the residual porosity of the ceramic.

The use of the uniaxial molding method in combination with powerful ultrasonic treatment and subsequent sintering of luminescent ceramics can be useful for improving the radiative properties of ceramics.

Funding

This study was supported by the Russian Science Foundation № 21-73-10100. In the paper, the equipment of the Centre for Collective Use CSU NMNT TPU was used, supported by the project of the Ministry of Education and Science of Russia № 075-15-2021-710 was used.

Conflict of interest

The authors declare that they have no conflict of interest.

References

[1] L. Zhang, B. Sun, L. Gu, W. Bu, X. Fu, R. Sun, T. Zhou, F.A. Selim, C. Wong, H. Chen. J. Alloys Compd., **455**, 425–432 (2018). DOI: 10.1016/j.apsusc.2018.05.133

[2] X. Li, C. Zhang, J. Chen, Q. Liu, Z. Bai, X. Liu, X. Mi, Cer. Int., **49**, 5489–5495 (2023). DOI: 10.1016/j.ceramint.2022.02.190

[3] Q.Q. Zhu, S. Li, Q. Yuan, H. Zhang, L. Wang. J. of the European Ceramic Society, **41** (1), 735–740 (2021). DOI: 10.1016/j.jeurceramsoc.2020.09.006

[4] M. Raukas, J. Kelso, Y. Zheng, K. Bergenek, D. Eisert, A. Linkov, F. Jermann. ECS J. Solid State Sc. and Technol., **2** (2), 3168–3176 (2013). DOI: 10.1149/2.023302jss

[5] T. Ji, T. Wang, H. Li, Q. Peng, H. Tang, S. Hu, A. Yakovlev, Y. Zhong, X. Xu, Adv. Opt. Mater., **10**, 2102056 (2022). DOI: 10.1002/adom.202102056

[6] X. Liu, H. Zhou, Z. Hu, X. Chen, Y. Shi, J. Zou, J. Li. Opt. Mater., **88**, 97–102 (2019). DOI: 10.1016/j.optmat.2018.11.031

[7] C. Cozzan, G. Lheureux, N. O'dea, E.E. Levin, J. Graser, T.D. Sparks. ACS Appl. Mater. Interfaces, **10**, 5673–5681 (2018). DOI: 10.1021/acsami.8b00074

[8] M. Kottaisamy, P. Thiyagarajan, J. Mishra, M.S. Ramachandra Rao. Mater. Res. Bull., **43** (7), 1657–1663 (2008). DOI: 10.1016/j.materresbull.2007.09.005

[9] G.H. Liu, Z.Z. Zhou, Y. Shi, Q. Liu, J.Q. Wan, Y.B. Pan. Mater. Lett., **139**, 480–482 (2015) DOI: 10.1016/j.matlet.2014.10.114

[10] C. Basu, M. Meinhardt-Wollweber, B. Roth. Adv. Opt. Tech., **2** (4), 213–321(2013). DOI: 10.1515/aot-2013-0031

[11] S. Li, Q. Zhu, D. Tang, X. Liu, G. Ouyang, L. Cao. J. Mater. Chem. C, **4** (37), 32–36 (2016). DOI: 10.1039/C6TC03215J

[12] S. Nishiura, S. Tanabe, K. Fujioka, Y. Fujimoto. Opt. Mater., **33** (5), 688–691 (2011). DOI: 10.1016/j.optmat.2010.06.005

[13] Q. Liu, J. Liu, J. Li, M. Ivanov, A. Medvedev, Y.P. Zeng, G.X. Jin, X.W. Ba, W.B. Liu, B.X. Jiang, Y.B. Pan, J.K. Guo. J. Alloys Compd., **616**, 81–88 (2014). DOI: 10.1016/j.jallcom.2014.06.013

[14] Y.R. Tang, S.M. Zhou, C. Chen, X.Z. Yi, Y. Feng, H. Lin, S. Zhang. Opt. Express, **23** (14), 17923–17928 (2015). DOI: 10.1364/OE.23.017923

[15] G.H. Liu, Z.Z. Zhou, Y. Shi, Q. Liu, J.Q. Wan, Y.B. Pan. Mater. Lett., **139**, 480–482 (2015). DOI: 10.1016/j.matlet.2014.10.114

[16] K. Liu, D. He, H. Wang, T. Lu, F. Li, X. Zhou. Scripta Mater., **66** (6), 319–322 (2012). DOI: 10.1016/j.scriptamat.2011.11.012

[17] R. Chaima, M. Kalina, James Z. Shen. J. Eur. Ceram. Soc., **27** (11), 3331–3337 (2007). DOI: 10.1016/j.jeurceramsoc.2007.02.193

[18] V.S. Kortov, S.V. Zvonarev, A.N. Kiryakov, D.V. Ananchenko. Radiation Measurements, **90**, 196–200 (2016). DOI: 10.1016/j.radmeas.2016.02.015

[19] O.L. Khasanov, E.S. Dvilis. Advances in Applied Ceramics, **107**, 135–141 (2008). DOI: 10.1179/174367508X297830

[20] E.S. Dvilis, O.L. Khasanov, V.M. Sokolov, Yu.P. Pokholkov. Method for compacting powder materials into articles and a mold for implementing the method U.S. Patent No. 6919041 B2 19 (2005).

[21] V.V. Osipov, O.L. Khasanov, V.A. Shitov, E.S. Dvilis, M.G. Ivanov, A.N. Orlov, V.V. Platonov, I.V. Vyukhina, A.A. Kachaev, V.M. Sokolov. Nanotech. Russia, **3** (7), 474–480 (2008). DOI: 10.1134/S1995078008070100

[22] O.L. Khasanov, E.S. Dvilis, E.F. Polisadova, S.A. Stepanov, D.T. Valiev, V.D. Paygin, D.V. Dudina. Ultrasonics Sonochem., **50**, 166–171 (2019). DOI: 10.1016/j.ultsonch.2018.09.013

[23] L.E. Muresan, A.I. Cadis, I. Perhaita, D.T. Silipas, L. Barbu Tudoran. Mater. Res. Bull., **68**, 295–301 (2015). DOI: 10.1016/j.materresbull.2015.03.063

[24] D. Valiev, T. Han, V. Vaganov, S. Stepanov. J. Phys. Chem. Solids, **116**, 1–6 (2018). DOI: 10.1016/j.jpcs.2018.01.007

[25] D. Valiev, T. Han, S. Stepanov, V. Vaganov, V. Paygin. Mater. Res. Express, **5**, 096201 (2018). DOI: 10.1088/2053-1591/aad609

[26] V.D. Paygin, S.A. Stepanov, D.T. Valiev, E.S. Dvilis, O.L. Khasanov, V.A. Vaganov, T.R. Alishin, M.P. Kalashnikov, A.E. Ilela. Nanotech. Russia, **14**, 113–117 (2019). DOI: 10.1134/S1995078019020113

[27] Y. Pan, M. Wu, Q. Su. Mater. Sci. Eng. B, **106**, 251–256 (2004). DOI: 10.1016/j.mseb.2003.09.031

[28] Y. Zorenko, T. Zorenko, V.V. Gorbenko, T. Voznyak, V. Savchyn, P. Bilski, A. Twardak. Opt. Mater., **34** (8), 1314–1319 (2012). DOI: 10.1016/j.optmat.2012.02.007

[29] A. Wiatrowska, W. Keur, C. Ronda. J. Lumin., **189**, 9–18 (2017). DOI: 10.1016/j.jlumin.2016.11.001

[30] J. Tang, Y. He, L. Hao, X. Xu et al. J. Mater. Res., **28** (18), 2598–2604 (2013). DOI: 10.1557/jmr.2013.228

[31] X. Wang, J. Li, P. Shi, W. Guan, H. Zhang. Opt. Mater., **46**, 432–437 (2015). DOI: 10.1016/j.optmat.2015.04.060

Translated by E.Potapova